UCLA
UCLA Previously Published Works

Title

Assessing the Bonding Properties of Individual Molecular Orbitals

Permalink

https://escholarship.org/uc/item/2zn9q038

Journal

The Journal of Physical Chemistry A, 119(51)

ISSN

1089-5639

Authors

Robinson, Paul J
Alexandrova, Anastassia N

Publication Date

2015-12-24

DOI

10.1021/acs.jpca.5b09687

Peer reviewed

Assessing the Bonding Properties of Individual Molecular Orbitals

Paul J. Robinson[†] and Anastassia N. Alexandrova[*,†,‡]

[†]Department of Chemistry and Biochemistry, University of California, Los Angeles California 90095, United States
[‡]California NanoSystems Institute, Los Angeles, California 90095, United States

ABSTRACT: Molecular orbitals (MOs), while one of the most widely used representations of the electronic structure of a system, are often too complex to intuit properties. Aside from the simplest of cases, it is not necessarily possible to visually tell which orbitals are bonding or antibonding along particular directions, especially in cases of highly delocalized and nontrivial bonding like metal clusters or solids. We propose a method for easily assessing and comparing the relative bonding contributions of MOs, by calculating their response to stress (e.g., compression). We find that this approach accurately describes relative bonding or antibonding character in both the simplest cases and provides new insight in more complex cases. We test the approach on four systems: H_2, Am_2, benzene, and the Pt_4 cluster. In exploring this methodology, a scheme became elucidated, for predicting changes in the ground electronic configuration upon compression, including changes in bonding order, angular momenta of occupied MOs, and trends in MO ordering. We note that the applications of this work go beyond simple molecules and could be straightforwardly extended to, for example, solids and their response to stress along the specific crystallographic plane. Additionally, predictions of structures and properties of chemical systems under stress could result from the emerging intuition about changes in the electronic structure.
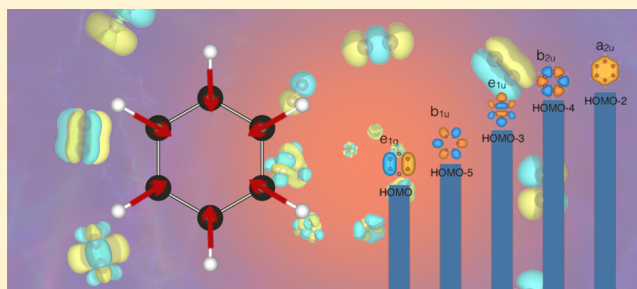
I. INTRODUCTION

Depending on the electronic geometry of a molecular orbital (MO), it can be considered bonding, nonbonding, or antibonding. Of course, this classification is not discrete, and there is variation in the bonding strength of orbitals. What really determines the bonding character of an orbital is its eigenenergy at the stable geometry of the system as compared to the eigenenergy of the same orbital in a greatly expanded geometry. Therefore, by sampling the MOs at two points along the right compression or expansion coordinate of a system one can semiquantitatively rank the orbitals by bonding character while only incurring the computational cost of two single point calculations.

The core of this approach depends on the predictable response of orbitals in systems under compression and can be traced back to a general chemistry exercise: we teach that in normal circumstances, the two-center-two-electron (2c-2e) bonds in simple diatomics fill in the order of σ, π, δ, φ, because of the diminishing quality of the atomic orbital (AO) overlap in this series. This pattern holds true even in very heavy diatomics, such as U_2, as demonstrated by Gagliardi and Roos.[1] The delocalized MOs in polyatomic molecules and clusters can also exhibit these types of overlap, i.e. σ, π, δ, φ.[2−8] Recall now that in the B_2 diatomic, an inversion of the σ_{2px} and π_{2pz} MOs is observed. This inversion happens because of the proximity of the nuclei in B_2. The 2p electrons avoid the most congested area of the already crowded internuclear space by populating the MO of higher angular momentum (π instead of σ). Noticeably, the effect goes beyond the simple diatomic and is

reflected also in the electronic structures of more complicated boron systems, such as clusters, when compared to the clusters of, for example, carbon or metals.[9,10] This beavior of AOs in B is representative of the general rule governing MO energy crossings, which we can take advantage of to facilitate bonding analysis.

To explore this methodology, we study the electronic states of a diverse set of diatomic and polyatomic molecules and clusters composed of main group-, d-, and f-elements. We show the manner in which the bonding pattern changes is predictable, quantifiable, and the result is a rapid way to determine which orbitals are most important to the bonding properties of a molecule. Additionally, we suggest an intuitive way to predict the qualitative changes in electronic configurations upon applied stress.

In our calculations, simple symmetry-preserving compressions and expansions of model molecules are employed in order not to favor any states through a sort of Jahn−Teller distortion. We do not go deeply into the treatment of multireference and relativistic effects, only pursuing a qualitative bonding picutre. We start from two extremes of diatomic molecules, H_2 and Am_2. The former is the simplest diatomic, and the latter can exhibit many different kinds of bonds formed by the seven unpaired f-electrons in Am. The electronic configurations of most diatomics under normal conditions are predictable in a
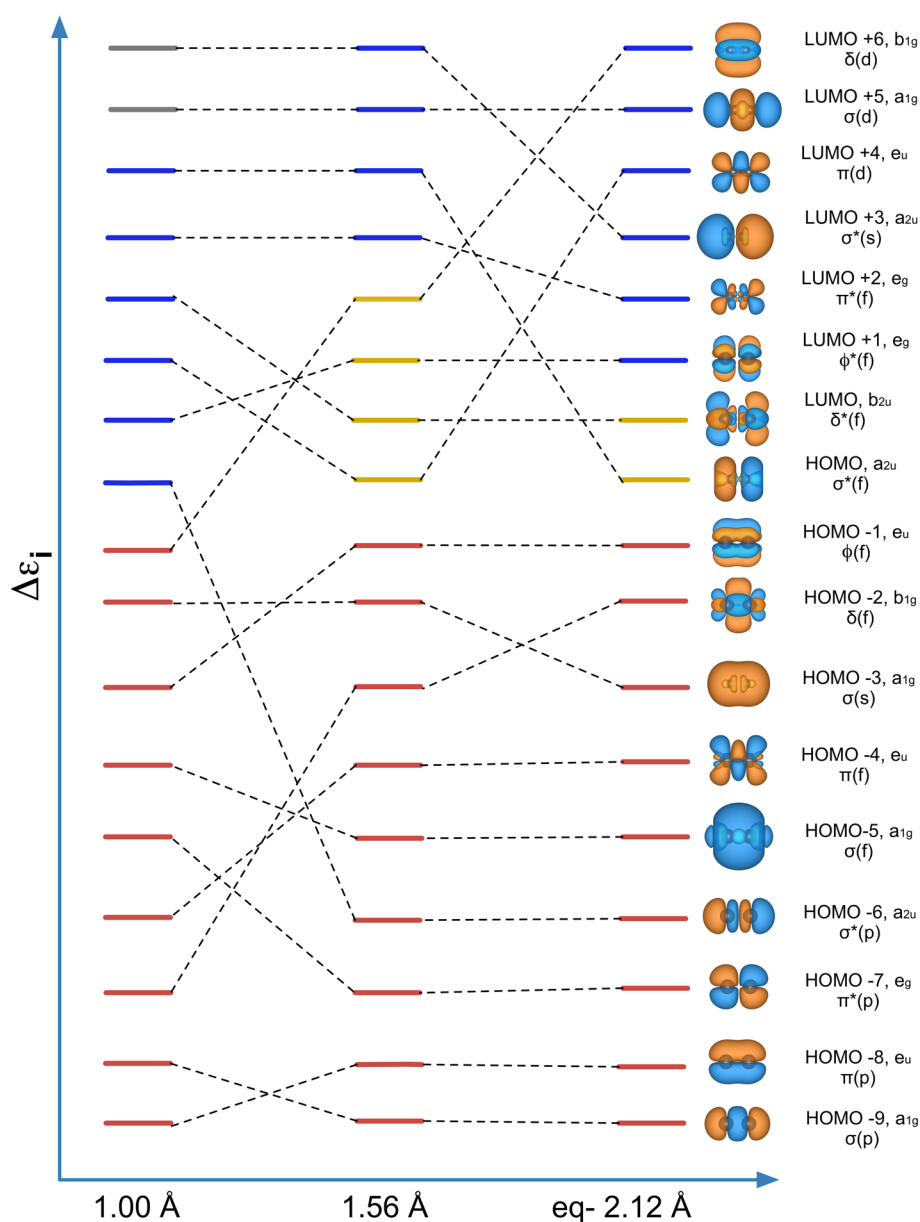
Figure 1. Valence MOs of Am$_2$ at equilibrium (eq) bond length (energies are not to scale). Red MOs are occupied, blue are unoccupied, yellow show partial occupancies (see section 2), and gray are off-scale-high in energy. All orbital energies are not to scale.

back-of-the-envelope fashion. We expect to be able to qualitatively reproduce the obvious bond strength ordering: $\sigma > \pi > \delta > \phi$. In more complex systems, this approach should allow us to both confirm the bonding properties of obvious bonding or antibonding orbitals and reveal the properties of orbitals in less obvious cases.

II. COMPUTATIONAL METHODS

The H$_2$ bond was treated in *Gaussian 09* with CISD and a cc-pV5Z basis set. An NBO analysis was performed on each of the H$_2$ calculations. For Am$_2$, the BLYP functional with the Stuttgart 1997 ECP basis set were used as implemented in *NWChem*.[11] The work of Takagi et al. demonstrated that the BLYP is quite accurate in predicting electronic structure for transition metal compounds.[12] The Stuttgart 1997 basis set was chosen because of a recent study on the uranium−uranium bond in U$_2$(OH)$_{10}$.[13] We explicitly included the 8s, 7p, 6d, and 4f atomic orbitals and assigned core potentials to 60 inner

orbitals. Fermi−Dirac smearing was included because of the close spacing of energy levels in metal systems. Pt$_4$ was treated with the PBE functional and the aug-cc-pVTZ-PP basis set. For benzene, single-point and optimization calculations were performed using *Gaussian 09*. CCSD(T) theory was used with a 6-31G basis set. Visualizatons of MOs were performed using the *VESTA* program.[14]

III. RESULTS AND DISCUSSION

1. Orbital Force Constant: k_ψ. Central to our methodology is a simple quantification of bonding. Each MO can be characterized by a constant; we call it k_ψ, describing the change in orbital eigenenergy when the molecular geometry is shifted away from equilibrium:

$$k_\psi = \frac{E_{n,l,0} - E_{n,l}}{r_0 - r} = \frac{\Delta E_{n,l}}{\Delta r}$$

It is defined as the change in energy of a specific MO as the molecule is compressed completely symmetrically. It is, in fact, just a representation of the slope of the correlation diagram but in symmetric scaling space. It is sometimes more desirable, depending on the system, to construct k_ψ values by expanding the molecule and changing the signs.

We must note that this method only works in conjunction with methods yielding orbital eigenenergies and thus cannot work with multiconfigurational methods. This is the case simply because our method directly analyzes the eigenenergies.

k_ψ is a quantitative measure of bonding character and is easily obtained from just two calculations near the equilibrium. The individual values of k_ψ are different at different geometric displacements and carry no meaning in isolation; however, the comparisons between the k_ψ values of different MOs provide a useful metric for determining relative bonding character/ strength. Even for MOs that look too complicated for an examination by the naked eye, the bonding or antibonding character can be revealed by the value of k_ψ.

One consequence of the fully symmetric scaling is that there is no prior knowledge of the types of bonds being compressed, meaning both weak and strong bonds will be compressed equally. This has the potential (as the stronger bonds get distorted into stranger shapes) to lead to errors in the results; however, in the current examples, this was not observed because our compressions and expansions were kept small.

The constant k_ψ is, in fact, related to the work of Pauling et al.,[15] who demonstrated that the bond order of a molecule is proportional to $\exp((r - r_0)/b))$, where b is an experimentally fitted parameter. By invoking k_ψ the aspect of nature behind this classical result is described.

2. H$_2$. H_2 is the smallest interesting entity we can consider. Although H_2^+ is smaller, it contains only one electron, and thus, our method of orbital analysis is not relevant. The effect of compression is modeled here by scaling the H−H distance down to a miniscule 0.1 Å (clearly not achievable in any modernly conceivable experimental setting). To follow the trend in electronic behavior, we also stretched the molecule to R(H−H) = 1 Å. Because there is only one occupied orbital in the natural singlet case of H_2, it is not a meaningful test of this method; however, the artificial triplet state of H_2 provides the simplest case for testing. This state is optimal for ranking the orbitals because it has 2 electrons and 2 orbitals. Its electronic configuration, $\sigma(1s)^1 \sigma*(1s)^1$, gives a very weak bonding effect due to the 2p-AOs mixing into the valence MOs. This mixing is stronger in the $1\sigma*(1s)$-MO. As compression occurs, the energies of the $1\sigma(1s)$- and $1\sigma*(1s)$-MOs change, and they do so at slightly different rates. In fact, all bonding orbitals (occupied and virtual) decrease in energy (up to a point of a very tight contraction), and antibonding orbitals increase. This energy spread is to be expected based on a simple particle-in-a-box model. The rising antibonding orbitals and the falling bonding orbitals of different angular momenta eventually cross, such that below 0.33 Å, the electronic configuration becomes $\sigma(1s)^1 \sigma(2s)^1$. Hence, the formal bond order increases from zero to 1. Overall, the effect in H_2 is fairly predictable and modest. It serves as a primitive preliminary verification that symmetric compression may be used to determine bonding strength. Bond order goes up, and therefore, the bonding states become relatively more stable and the antibonding state become relatively less stable.

3. Am$_2$. Am_2 is a more exciting example. It is optimal for examining simple higher order bonds because of the half-full f-shell in Am,[16] and the resultant ability of the f-AOs to exhibit all kinds of bonding overlaps up to ϕ. It is understood that a multireference and truly relativistic treatment of Am_2 would be more accurate, but that is an involved study in its own right. Here, our purpose is a qualitative analysis of simple high-order bonding rather than specific properties of Am_2; therefore, we rely on DFT and modest basis sets for the current pursuit.

We examined the structures of Am_2 between the equilibrium bond length (calculated to be 2.12 Å) and 1.00 Å. At equilibrium, the structure takes on a form that matches the back-of-the-envelope predictions, filling the MOs in the order of $\sigma \rightarrow \pi \rightarrow \delta \rightarrow \phi$-: $(\sigma(p))^2 (\pi(p))^4 (\pi*(p))^4 (\sigma*(p))^2 (\sigma(f))^2 (\pi(f))^4 (\sigma(s))^2 (\delta(f))^4 (\varphi(f))^4 (\sigma*(f))^2$. Aside from having a calculated Mulliken bond order of 7.17, there is nothing novel about this molecule. However, as the Am−Am distance shrinks, the same pattern which appeared in H_2 appears. Again, the bonding MOs generally become more stable and antibonding MOs become less stable, and the rate of the MO-energy change depends on the angular momentum of the MO. The electron−electron repulsion becomes unfavorably high in lower angular momentum MOs upon compression, while an increased number of nodes in an MO becomes more favorable, allowing for a greater radial spread of electrons. Orbital shifts due to these changes are reported in Figure 1.

There is a clear pattern underlying this behavior. As the internuclear distance shrinks, the bonding MOs with a greater spread away from the bond axis become more stable, and they do so faster than the bonding orbitals of lower angular momenta. The higher angular momentum bonding MOs generally get populated more readily, displacing several lower angular momentum antibonding states out of the valence manifold, sometimes favoring a high-nodality ϕ bond over $\sigma*$ formed by the same type of AOs. The bond order then increases accordingly.

The k_ψ values of Am_2 (Table 1) clearly show the equilibrium bonding character of σ, π, δ, and ϕ-bonds. The σ-bond has a k_ψ

Table 1. Selected k_ψ Values[a]

Am$_2$		C$_6$H$_6$		Pt$_4$	
MO	k_ψ (eV/Å)	MO	k_ψ (eV/Å)	MO	k_ψ (eV/Å)
σ(f)	10.096	e_{2g}	17.355	$3a_1$	3.4951
π(f)	8.837	e_{1g}	19.375	$2a_1$	3.1441
δ(f)	7.286	e_{1u}	29.211	a_2	−2.6976
ϕ(f)	1.702	a_{2u}	35.912	e_1	−2.9076

[a]In the case of Am_2, they accurately reproduce the obvious trend in bond strength. For the benzene system, note the decrease in bonding character between the different MO components of the aromatic system. Finally, the relative energies of Pt_4 at different R(Pt−Pt), approximated forces acting on Pt_4 to lead to the given compression, and selected-MO ordering.

value about 6 times more than the ϕ-bond. Valence orbitals of higher angular momenta also show smaller k_ψ, because the AO-overlap becomes increasingly weaker.

4. C$_6$H$_6$−Benzene. We now move to 2-D polyatomic structures using benzene to further demonstrate the usefullness of symmetry-preserving expansion in determining bonding character.

Figure 2 depicts the familiar valence MOs of benzene at its calculated optimal geometry, R(C−C) = 1.417 Å, and R(H−C) = 1.096 Å, and the changes in the MO order under stress. To observe the orbital transfers, the optimized bond lengths were
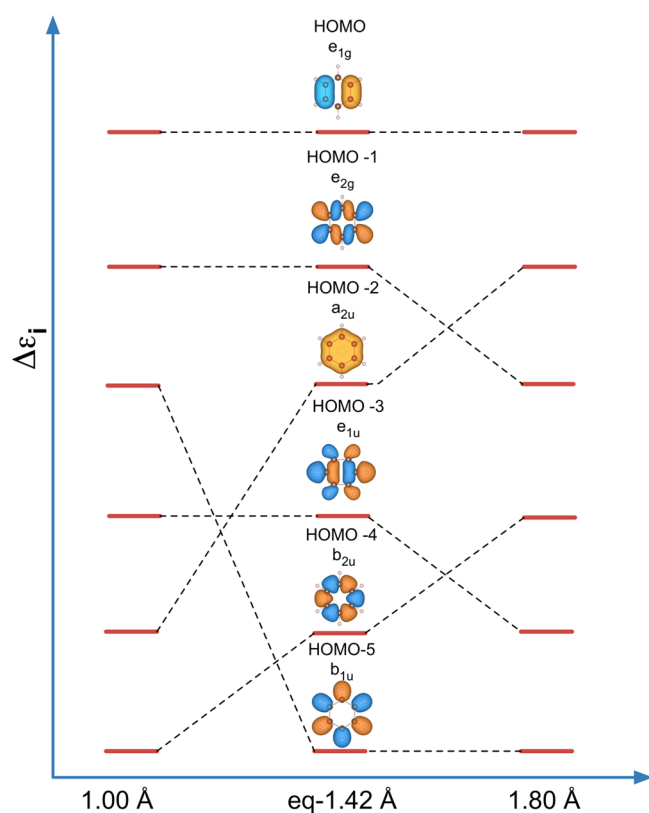
Figure 2. Relative orderings of valence MOs of benzene at equilibrium, expansion, and compression. Orbital energies are not to scale.

scaled both up and down. Consistent with the previous discussion, upon geometric contraction, the more antibonding orbitals tend to rise in energy, and bonding MOs sink in energy. The inverse is true when the system is expanded. At the dissociation limit, the energy differences between the bonding and corresponding antibonding states vanish. We restricted the compressions to a minimum value of 0.5 Å. Within this range, we did not observe any previously virtual orbitals entering into the valence manifold. This is not surprising, because for main group elements, the orbitals of large angular momenta are very high in energy at equilibrium. However, the observed trends suggest that upon even further compression, we could see the switching of occupied and vacant MOs, perhaps even breaking the aromatic character of the system.

The e_{2g} MO is the least bonding valence MO formed by in-plane σ-overlap, and it rises by 0.025 eV when R(C−C) is compressed to 1.00 Å. Conversely, the more bonding e_{1u} orbital decreases by 0.098 eV under the same compression. Neither the e_{1u} nor the e_{2g} MO are strongly bonding, and so their energy shifts are moderate. The b_{2u} and b_{1u} MOs are visually similar and yet they exhibit very different bonding properties when the C−C bond is compressed to 1.00 Å. The b_{2u} MO is part of the system of MOs that make up what would be simply described as C−C single bonds. This MO sinks by 0.163 eV because of its fully C−C bonding character. The b_{1u} orbital, on the other hand, increases in energy by 0.028 eV. This is, of course, because it is fully antibonding with respect to the carbon ring. The bonding character it exhibits with the hydrogens is dwarfed in comparison to the repulsion between the carbon atoms. Finally, we consider the e_{1g} and a_{2u} orbitals, which together are responsible for the aromaticity of benzene. Under compression, the e_{1g} MO sinks by 0.098 eV, though it remains the HOMO of the system under both expansion and
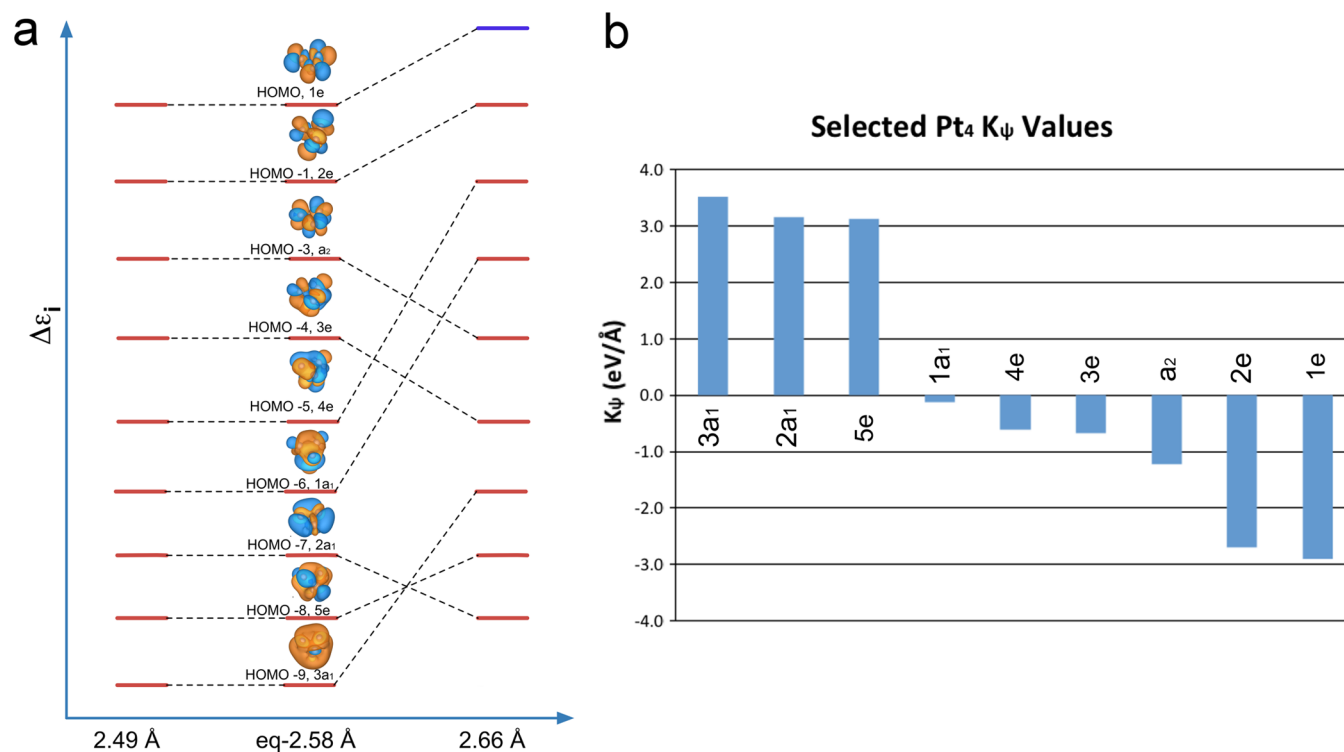
Figure 3. (a) Valence MOs of Pt$_4$. The expansion over the same distance creates a great effect, whereas the considered compression led to MO shifts but no orbital switching. Orbital energies are not to scale. (b) The k_ψ values of each MO.

compression. The a_{2u} decreases in energy by 0.252 eV, more than double the change in the partially bonding e_{1g}. This relationship is in-line with the increased bonding character in a_{2u} over e_{1g}.

If we use k_{ψ} as a measure, the character of orbitals is much more easily intuited (see Table 1). For example, among the delocalized π-MOs in benzene, the highest value of k_{ψ} belongs to the a_{2u} orbital (the fully bonding π-MO of the aromatic system). The e_{1g} HOMO orbitals have a k_{ψ} of approximately half the a_{2u} orbitals. This decrease in k_{ψ} correlates directly to the greater antibonding character of the e_{1g} MO.

5. Pt$_4$. Pt$_4$ is an example of a 3-D system with delocalized bonding formed by d- and s-AOs.[17] The goal of studying it is to elucidate the changes in the bonding pattern in 3-D. Pt$_4$ at equilibrium is tetrahedral. There is a single bonding σ-MO formed by the 6s-AOs on all four atoms, and the electron pair in this MO is promoted from the formerly full set of 5d-AOs, as is shown in Figure 3a. This type of delocalized bonding can be labeled as 3-D σ-aromatic, according to the $(4n + 2)$ Huckel's electron counting rule ($n = 0$).[17,18] The hole remaining in the set of MOs formed by 5d-AOs is also bonding.[17] We note that it is important not take into account the possible changes in geometry or spin state of the cluster upon compression.

In general, delocalized MOs in 3-D start looking more complicated, and it is not always clear whether an MO is bonding or antibonding. However, just as in the case of Am$_2$, the orbitals of compressed Pt$_4$ begin to diverge, and it is anticipated that the antibonding MOs become less energetically favorable, and all (occupied and virtual) bonding MOs become more favorable. Table 1 shows the relative energies and orbitals ordering at compression and also expansion of the cluster geometry. At the considered compression, no new orbital recruitment was found, and further compression resulted in poor SCF convergence, possibly indicating the onset of strong multireference character. Under expansion, however, the MO-rearrangements can be seen. As shown in Figure 3b, even at small compression and expansion values, the shifts in orbital energies are remarkable. For example, the a_2 MO, a fully antibonding MO with four nodal planes, increases in energy by 0.072 eV under compression. The $3a_1$ MO is the bonding σ-MO in the cluster that contributes to its σ-aromaticity. Upon compression to R(Pt−Pt) = 2.49, its energy lowers by 0.234 eV. Upon even a small expansion, however, it rises in energy dramatically. As the molecule begins to be compressed more, additional bonding character is provided by the $2a_1$ and $5e$ MOs.

A clear and intuitive pattern emerges from the preceding case studies: MOs that are bonding along the direction of distortion in a molecule should decrease in energy upon compression and rise in energy upon expansion along that direction, and antibonding MOs should exhibit the opposite behavior. The speed with which the MO-energies change depends on the angular momentum of the MO.

Now, it is also apparent that it is possible to engage in the reverse activity: by knowing how the energy of an orbital behaves upon a small compression or expansion, one can guess its bonding character along the direction of distortion. For example, the convoluted-appearing $3e$ MO in Pt$_4$ responds to expansion by becoming more stable. This indicates that it has more antibonding character than bonding character.

IV. CONCLUSIONS

In conclusion, we devised a descriptor for MOs, k_{ψ}, which contains the information about the relative bonding character of a particular MO. In addition, k_{ψ} is a convenient quantity in that it is trivially calculated.

The constant is expected to be especially useful for bonding analysis of complex systems, including materials, where bonding or antibonding character are often hard to understand from visual examination. If applied to a solid-state system, k_{ψ} could accurately predict the bonding character of a specific band or localized orbital. Additionally, although in this work the applied stress was isotropic, it does not generally have to be. The bonding character of an MO can be also elucidated along a particular direction in a molecule or a specific crystallographic plane in a material, elucidating the anisotropy of materials response to stress and chemical bonding reasons for it.

■ AUTHOR INFORMATION

Corresponding Author
*E-mail: ana@chem.ucla.edu.
Notes
The authors declare no competing financial interest.

■ REFERENCES

(1) Gagliardi, L.; Roos, B. O. Quantum Chemical Calculations Show That The Uranium Molecule U$_2$ Has A Quintuple Bond. *Nature* **2005**, *433*, 848−851.

(2) Alexandrova, A.; Boldyrev, A. Sigma-Aromaticity And Sigma-Antiaromaticity In Alkali Metal And Alkaline Earth Metal Small Clusters. *J. Phys. Chem. A* **2003**, *107*, 554−560.

(3) Zubarev, D.; Averkiev, B.; Zhai, H.; Wang, L.; Boldyrev, A. Aromaticity And Antiaromaticity In Transition-Metal Systems. *Phys. Chem. Chem. Phys.* **2008**, *10*, 257−267.

(4) Sergeeva, A.; Boldyrev, A. Delta-Bonding In The [Pd$_4$(M$_4$-C$_9$H$_9$)(M$_4$-C$_8$H$_8$)]$^+$ Sandwich Complex. *Phys. Chem. Chem. Phys.* **2010**, *12*, 12050−12054.

(5) Zhai, H.; Averkiev, B.; Zubarev, D.; Wang, L.; Boldyrev, A. Delta Aromaticity In [Ta$_3$O$_3$]$^-$. *Angew. Chem., Int. Ed.* **2007**, *46*, 4277−4280.

(6) Minkin, V.; Glukhovtsev, M.; Simkin, B. *Aromaticity and Antiaromaticity Electronic and Structural Aspects*; Wiley-Interscience: New York, 1994.

(7) Boldyrev, A.; Wang, L. All-Metal Aromaticity And Antiaromaticity. *Chem. Rev.* **2005**, *105*, 3716−3757.

(8) Galeev, T.; Boldyrev, A. Recent Advances In Aromaticity And Antiaromaticity In Transition-Metal Systems. *Annu. Rep. Prog. Chem., Sect. C: Phys. Chem.* **2011**, *107*, 124−147.

(9) Alexandrova, A.; Boldyrev, A.; Zhai, H.; Wang, L. All-Boron Aromatic Clusters As Potential New Inorganic Ligands And Building Blocks In Chemistry. *Coord. Chem. Rev.* **2006**, *250*, 2811−2866.

(10) Huynh, M.; Alexandrova, A. Persistent Covalency And Planarity In The B$_n$Al$_{6-n}^{2-}$ And LiB$_n$Al$_{6-n}^-$ (n = 0−6) Cluster Ions. *J. Phys. Chem. Lett.* **2011**, *2*, 2046−2051.

(11) Valiev, M.; Bylaska, E.; Govind, N.; Kowalski, K.; Straatsma, T.; Van Dam, H.; Wang, D.; Nieplocha, J.; Apra, E.; Windus, T.; de Jong, W. NWChem: A Comprehensive And Scalable Open-Source Solution For Large Scale Molecular Simulations. *Comput. Phys. Commun.* **2010**, *181*, 1477−1489.

(12) Takagi, N.; Krapp, A.; Frenking, G. On The Nature Of Homo- And Hetero-Dinuclear Metal−Metal Quadruple Bonds — Analysis Of

The Bonding Situation And Benchmarking DFT Against Wave Function Methods. *Can. J. Chem.* **2010**, *88*, 1079−1093.

(13) Penchoff, D. A.; Bursten, B. E. Metal-Metal Bonding In The Actinide Elements: Conceptual Synthesis Of A Pure Two-Electron U-U F Delta Single Bond In A Constrained Geometry Of $U_2(OH)_{10}$. *Inorg. Chim. Acta* **2015**, *424*, 267−273.

(14) Momma, K.; Izumi, F. VESTA: A Three-Dimensional Visualization System For Electronic And Structural Analysis. *J. Appl. Crystallogr.* **2008**, *41*, 653−658.

(15) Pauling, L. Atomic Radii And Interatomic Distances In Metals. *J. Am. Chem. Soc.* **1947**, *69*, 542−553.

(16) Cotton, S. *Lanthanide and Actinide Chemistry*; Wiley: Chichester, England, 2006.

(17) Ha, M.; Dadras, J.; Alexandrova, A. Rutile-Deposited Pt-Pd Clusters: A Hypothesis Regarding The Stability At 50/50 Ratio. *ACS Catal.* **2014**, *4*, 3570−3580.

(18) Zhang, J.; Alexandrova, A. The Golden Crown: A Single Au Atom That Boosts The CO Oxidation Catalyzed By A Palladium Cluster On Titania Surfaces. *J. Phys. Chem. Lett.* **2013**, *4*, 2250−2255.